Cryogenic Operation of a Silicon-Organic Hybrid (SOH) Modulator at 50 Gbps and 4 K Ambient Temperature

A. Schwarzenberger[1], A. Kuzmin[1,2], C. Eschenbaum[1,3], C. Füllner[1], A. Mertens[1,3], L.E. Johnson[4], D. L. Elder[4], S. R. Hammond[4], L. Dalton[5], S. Randel[1], W. Freude[1], and C. Koos [1,3]

[1] Institute of Photonics and Quantum Electronics (IPQ) / Institute of Microstructure Technology (IMT), Karlsruhe Institute of Technology (KIT), Karlsruhe, Germany
[2] Laboratory for Applications of Synchrotron Radiation (LAS), Karlsruhe Institute of Technology (KIT), Karlsruhe, Germany
[3] SilOriX GmbH, Karlsruhe, Germany
[4] NLM Photonics, Seattle, WA, USA
[5] Department of Chemistry, University of Washington, Seattle, USA
adrian.schwarzenberger@kit.edu; christian.koos@kit.edu

Abstract *We demonstrate cryogenic operation of a silicon-organic hybrid (SOH) Mach-Zehnder modulator. The device is based on a dedicated material formulation and allows for 50 Gbps on-off-keying (OOK) at 4 K - a record-high line rate generated by an MZM at this temperature.* ©2022 The Authors

Introduction

Novel computing paradigms using quantum approaches or electronic circuits at cryogenic temperatures are expected to overcome the limitations of conventional processors [1–4]. A critical aspect of the underlying system architectures is the communication between the cryogenic processing core, which is often operated at liquid-helium temperatures around 4K, and the room-temperature (RT) environment. In this context, optical links have unique advantages over electrical connections, offering high transmission rates, good thermal isolation, immunity to thermal noise, and robustness with respect to electromagnetic interference [4]. On a device level, such links require highly efficient electro-optic (EO) modulators that can be operated at cryogenic temperatures and that can convert low-level electrical stimulus signals into optical signals with lowest possible power dissipation.

Over the previous years, several EO modulator concepts have been investigated with respect to cryogenic operation, including conventional lithium-niobate Mach-Zehnder modulators (MZM) [6], *p-n*-type silicon photonic (SiP) devices based on carrier injection or depletion in ring-resonator structures [9-11], barium-titanate-based racetrack resonators and MZM [8], as well as heterogeneously integrated InP-on-Si devices [5]. However, the data rates demonstrated for cryogenic transmitters so far were limited to 20 Gbit/s with unspecified bit-error ratios (BER), achieved with Si ring [5, 9-11] and $BaTiO_3$-on-Si [8] racetrack resonators, both operated at drive voltages of 1.5 V or more. In this context, it should be noted that the transmission speed of resonant cryogenic devices is eventually limited by the Q-factor of the underlying resonator, leading to a fundamental trade-off between modulation efficiency and speed. MZMs, on the other hand, are not subject to this trade-off, but the modulation voltages so far demonstrated for cryogenic MZMs still exceed 5 V while the data rate was limited to 5 Gbps [6].

In this paper, we overcome these limitations by demonstrating a highly efficient MZM, suited for cryogenic transmission with sub-1 V drive voltages. Our device relies on the silicon-organic hybrid (SOH) integration concept and combine slot waveguides with dedicated three-level doping profiles with a special formulation of JRD1 mixed with PMMA, an organic electro-optic material that does not exhibit any strain-related cracking upon cool-down to cryogenic temperatures. We demonstrate the viability of the devices in cryogenic transmission experiments with line rates of up to 60 Gbit/s and analyze the resulting BER performance. Using an MZM with a 50 Ω termination, we demonstrate 50 Gbit/s signaling with a BER of 7×10^{-4} at a peak-to-peak drive voltage of 1.6 V_{pp}. For 40 Gbit/s, we do not find any errors in our recordings of 8×10^6 samples once the drive voltages exceed 1.1 V. Allowing for BER corresponding to standard forward-error-correction (FEC) with 7 % and 20 % overhead, the drive voltages can be reduced to 700 mV and 500 mV, corresponding to energy dissipations of 61 fJ/bit and 31.3 fJ/bit, respectively. To the best of our knowledge, our results represent the highest data rates hitherto demonstrated with an electro-optic modulator at 4 K, while our MZM drive voltages are even smaller than the 1.5 V and the 1.7 V used in high-speed ring modulators at lower data rates [5, 8-11]. Note also that the data rates in the current experiments are still largely limited by the RF signal path into the cryostat and that both the material and the device SOH design leave vast room for further improvement, hence paving a path towards highly efficient optical interconnects in cryogenic supercomputers.

Device and packaging concept for cryo operation: The concept of the SOH device used in our

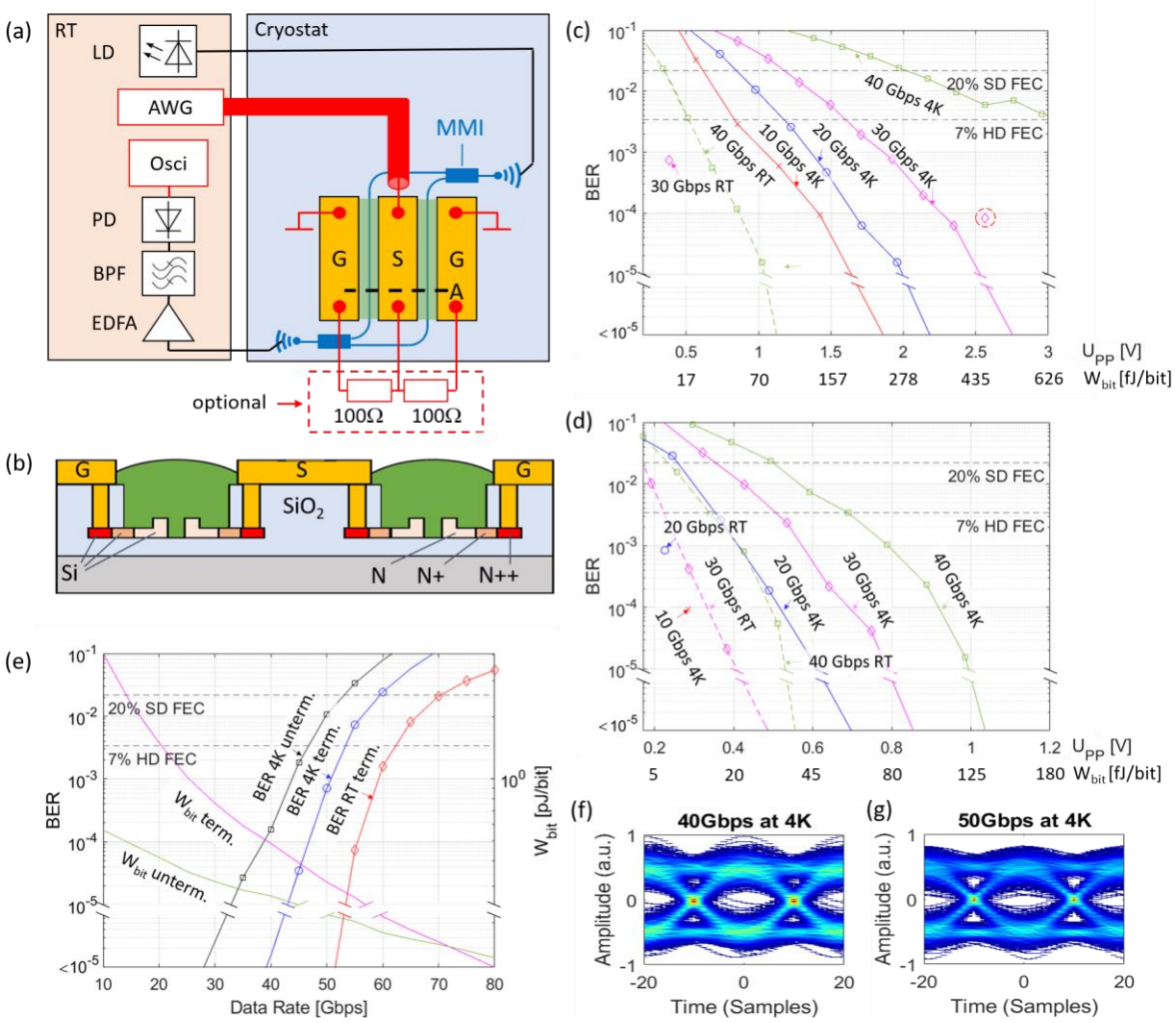

Fig. 1: SOH device principle, experimental setup and results. (a) Experimental setup. The electrical package can be placed in a cryostat such that measurements both at 4 K and room temperature are possible. An Arbitrary Waveform Generator (AWG) in combination with a RF amplifier generates a Pseudo Random Bit Sequence (PRBS). The Laser Diode (LD) provides the laser light, which is coupled to the modulator via grating couplers. The light is split into the two arms of the MZM by a Multimode Interferometer coupler (MMI). The modulated light is amplified in an EDFA, filtered (BPF) and detected in a Photodiode (PD) connected to a high-speed oscilloscope. The waveform is captured and processed using offline DSP in order to calculate the BER. (b) Cross section of the SOH MZM along the dashed line A in (a). Each MZM arm features a silicon photonic (SiP) slot wave-guide, which is filled by the organic EO material mixture JRD1:PMMA. The rails are electrically connected to the ground-signal-ground (GSG) transmission line via Si slabs and vias. The Si rails feature three doping level concentrations N, N+ and the contact doping N++ [12]. Sweep of the drive voltage (U_{pp}) of the unterminated (unterm.) (c) and terminated (term.) (d) modulator for 10, 20, 30 and 40 Gbps at both RT and 4K. We attribute the significantly decrease in performance of the unterminated device at 4K to damage of the package of the device. (f) Data rate sweep for both the terminated and unterminated device at RT and 4K. The calculated energy dissipation per bit in (c), (d) and (e) is based on the method outlined in [15]. (f) and (g) depict eye diagrams generated after the DSP chain for the terminated device. In (f) an eye diagram for a 40Gbps signal with a drive voltage of 1.08 V and an electrical power dissipation of 147 fJ/bit is shown. The BER is below the detection limit with a 99% confidence level of 1e-5. (g) shows an eye diagram for a 50 Gbps signal with a drive voltage of 1.58 V and an electrical power dissipation of 250 fJ/bit. The BER is 7e-4 with a 99% confidence level of 8.3e-6.

demonstration and the corresponding experimental setup are is illustrated in Fig. 2(a) and (b). The optical carrier is generated by a laser operating at room temperature in the C-band with a power of 10dBm. The light is coupled to the SiP waveguides (blue) of the SOH MZM via a grating coupler (GC). The light is split into the two arms of the SOH MZM by a multi-mode interference coupler (MMI) and is recombined by another MMI at the output. At the output, the data signal is coupled to the egress fiber via a second GC and transported back to the RT receiver, consisting of an erbium-doped fiber amplifier (EDFA), a band-pass filter (BPF), a high-speed photodiode (43 GHz), and a real-time oscilloscope (110 GHz Keysight Infiniium URX1104A) for recording the received waveforms. Figure 2(b) depicts the cross section of the two MZM arms. Each arm contains an SOH phase shifter consisting of a SiP slot waveguide. The waveguide is formed by two Si rails (width 240 nm), separated by a 140 nm-wide slot. Thin doped Si slabs connect the rails to a ground-signal-ground (G-S-G) transmission line, which is electrically connected to the top

metal layer by vias. The Si slabs have three regions with different doping concentrations, where lower concentrations are used in the vicinity of the waveguide core and higher concentrations are used in the more distant regions of the slab, see [12] for details. The doping profile offers low optical losses due to free-carrier absorption and in the same time increases the RC bandwidth and lessens the impact of carrier freeze-out [12].
Previous studies already indicated that EO organic materials could be used at cryogenic temperatures [13] and serve as an EO-tuneable cladding for SiP quantum transduction devices [14].
The highly efficient organic EO material JRD1 is mixed with PMMA and deposited on the slot waveguides in a post-processing step [12]. Highly efficient EO modulation with voltage-length products down to 0.32 Vmm was demonstrated at room temperature for pure JRD1 [16] and down to 1.0 Vmm for JRD1:PMMA mixture. For RF packaging, the SiP chip is connected to two ceramic PCBs with coaxial 1.85 mm ("V") end launchers, which ensure easy connection to cryogenic coaxial cables. The PCBs are laser etched on an alumina substrate (Al_2O_3) covered by a 3 µm-thick electroplated Au layer. The PCB traces are designed as tapered 50 Ω coplanar GSG transmission lines (TL). For assembly, the SiP chip is first glued on a copper-tungsten poling sub-mount using a silver filled two-component epoxy. Subsequent to the poling of the SOH device the SiP chip on the copper sub-mount and the two PCBs are aligned on a common aluminium sub-mount and mechanically fixed. The electrodes of the modulators are connected to the PCB traces at both ends using Au ribbon bonds (length ~ 200 µm).

Device characterization at 4 K

A custom-build closed-cycle cryogenic probe station was used to characterize the device at 4K. It is based on a pulsed-tube cooler TransMIT PTD 406C with vibration-isolation platform and two vacuum-compatible 3-axis piezo manipulators for alignment of fiber probes and coupling light into SiP-chip. With a device length of L = 1mm, this leads to π-voltage-length products of $U_\pi L$ = 1.99 Vmm at room temperature and of $U_\pi L$ = 2.0 Vmm at 4 K. With an optimized poling recipe of JRD1:PMMA mixture we were able to achieve $U_\pi L$ as low as 1.0 Vmm at 300 K, but these devices are yet to be measured at 4 K.

To demonstrate the viability of our MZM for data transmission at cryogenic temperatures, we operate the device at 4 K with non-return to zero (NRZ) on-off-keying (OOK) signals at bit rates of up to 50 Gbps, see Fig. 2 (e) for a sketch of the experimental setup. The signals were recorded and passed through a digital signal processing (DSP) chain consisting of Frontend Corrections, Timing Recovery and a Sato Equalizer for impairment compensation. Afterwards the BER was calculated.
From Fig. 2 we see that drive voltages at 4K are about factor 2 higher for the same BER and data rates. This we attribute to a reduced conductivity of the doped slabs affected by carrier freeze-out. Further optimization of doping profile will allow to reduce SOH drive voltages for cryogenic operation.

Summary and outlook

We have demonstrated cryogenic operation of a silicon-organic hybrid (SOH) Mach-Zehnder modulator (MZM) with slot waveguides and optimized two-level doping profile of the Si slabs which couples RF mode into the slot region and allows to mitigate carrier freezout at 4K. The devices exhibit π-voltages of less than 2 V and $U_\pi L$-products below 2 Vmm both at room temperature and at 4 K.
We demonstrate 50 Gbit/s OOK data transmission with a BER of 7×10^{-4} at a peak-to-peak drive voltage of 1.6 Vpp, and error-free 40 Gbit/s for U_{pp} of 1.1 V. Assuming BER that corresponds 7 % and 20 % FEC overhead, the drive voltages can be reduced to 700 mV and 500 mV, corresponding to energy dissipations of 61 fJ/bit and 31.3 fJ/bit, respectively. To the best of our knowledge, our results represent the highest data rate for an electro-optic modulator at 4 K to this date.

Acknowledgements: This research has been funded by the European Research Council (ERC Consolidator Grant 'TeraSHAPE', # 773248), by the EU project "TeraSlice" (863322), by the IARPA SuperCables Program ICENET (W911NF1920114), by the Deutsche Forschungsgemeinschaft (DFG, German Research Foundation) via the DFG projects HIPES (383043731) and PACE (403188360) and via the Excellence Cluster 3D Matter Made to Order (EXC-2082/1 – 390761711), by the BMBF project SPIDER (01DR18014A), and by the Alfried Krupp von Bohlen und Halbach Foundation.

References

[1]. Tolpygo, S. K. "Superconductor digital electronics: Scalability and energy efficiency issues" (Review Article), *Low Temperature Physics*, AIP Publishing, 2016, 42, 361-379 DOI: 10.1063/1.4948618.

[2]. Likharev, K. & Semenov, V. "RSFQ logic/memory family: a new Josephson-junction technology for sub-terahertz clock-frequency digital systems", *IEEE Transactions on Applied Superconductivity*, Institute of Electrical and Electronics Engineers (IEEE), 1991, 1, 3-28. DOI: 10.1109/77.80745.

[3]. Castelvecchi, D. "Quantum computers ready to leap out of the lab in 2017", *Nature*, Springer Science and Business Media LLC, 2017, 541, 9-10. DOI: 10.1038/541009a.

[4]. K McCammon, K.; Morse, J.; Masquelier, D.; McConaghey, C.; Garrett, H.; Hugenberg, K. et al. “Fiber optic transceiver for interfacing digital superconducting electronics”, article, March 1, 1994; California. (https://digital.library.unt.edu/ark:/67531/metadc1316210/ : accessed September 4, 2022), University of North Texas Libraries, UNT Digital Library, https://digital.library.unt.edu ; crediting UNT Libraries Government Documents Department.

[5]. Pintus, P.; Singh, A.; Xie, W.; Ranzani, L.; Gustafsson, M. V.; Tran, M. A.; Xiang, C.; Peters, J.; Bowers, J. E. & Soltani, M. “Ultralow voltage, High-speed, and Energy-efficient Cryogenic Electro-Optic Modulator”, *arXiv*, 2022. DOI: 10.48550/arXiv.2207.03570 .

[6]. Youssefi, A.; Shomroni, I.; Joshi, Y. J.; Bernier, N. R.; Lukashchuk, A.; Uhrich, P.; Qiu, L. & Kippenberg, T. J. “A cryogenic electro-optic interconnect for superconducting devices”. *Nature Electronics*, Springer Science and Business Media LLC, 2021, 4, 326-332. DOI: 10.1038/s41928-021-00570-4.

[7]. Chakraborty, U.; Carolan, J.; Clark, G.; Bunandar, D.; Gilbert, G.; Notaros, J.; Watts, M. R. & Englund, D. R. “Cryogenic operation of silicon photonic modulators based on the DC Kerr effect”, *Optica*, The Optical Society, 2020, 7, 1385. DOI: 10.1364/OPTICA.403178.

[8]. Eltes, F.; Villarreal-Garcia, G. E.; Caimi, D.; Siegwart, H.; Gentile, A. A.; Hart, A.; Stark, P.; Marshall, G. D.; Thompson, M. G.; Barreto, J.; Fompeyrine, J. & Abel, S. “An integrated optical modulator operating at cryogenic temperatures” *Nature Materials* , 2020, 19, 1164-1168. DOI: 10.1038/s41563-020-0725-5.

[9]. Gehl, M.; Long, C.; Trotter, D.; Starbuck, A.; Pomerene, A.; Wright, J. B.; Melgaard, S.; Siirola, J.; Lentine, A. L. & DeRose, C. ”Operation of high-speed silicon photonic micro-disk modulators at cryogenic temperatures”, *Optica*, The Optical Society, 2017, 4, 374. DOI: 10.1364/OPTICA.4.000374

[10]. Gevorgyan, H.; Khilo, A.; Orden, D. V.; Onural, D.; Yin, B.; Wade, M. T.; Stojanović, V. M. & Popović, M. A. “Cryo-Compatible, Silicon Spoked-Ring Modulator in a 45nm CMOS Platform for 4K-to-Room-Temperature Optical Links”, *2021 Optical Fiber Communications Conference and Exhibition (OFC),* 2021, 1-3. URL: https://ieeexplore.ieee.org/document/9489439 :accessed 4 September 2022.

[11]. Lee, B. S.; Kim, B.; Freitas, A. P.; Mohanty, A.; Zhu, Y.; Bhatt, G. R.; Hone, J. & Lipson, M. ”High-performance integrated graphene electro-optic modulator at cryogenic temperature”, *Nanophotonics*, Walter de Gruyter GmbH, 2020, 10, 99-104, DOI: 10.1515/nanoph-2020-0363.

[12]. Zwickel, H.; Singer, S.; Kieninger, C.; Kutuvantavida, Y.; Muradyan, N.; Wahlbrink, T.; Yokoyama, S.; Randel, S.; Freude, W. & Koos, C. “Verified equivalent-circuit model for slot-waveguide modulators”, *Optics Express*, The Optical Society, 2020, 28, 12951 DOI: 10.1364/OE.383120

[13]. Witmer, J. D.; McKenna, T. P.; Arrangoiz-Arriola, P.; Laer, R. V.; Wollack, E. A.; Lin, F.; Jen, A. K.-Y.; Luo, J. & Safavi-Naeini, A. H. “A silicon-organic hybrid platform for quantum microwave-to-optical transduction”, *Quantum Science and Technology*, IOP Publishing, 2020, 5, 034004, DOI: 10.1088/2058-9565/ab7eed.

[14]. Park, D.; Yun, V.; Luo, J.; Jen, A.-Y. & Herman, W., “EO polymer at cryogenic temperatures”, *Electronics Letters*, Institution of Engineering and Technology (IET), 2016, 52, 1703-1705. DOI: 10.1049/el.2016.1406

[15]. Koeber, S.; Palmer, R.; Lauermann, M.; Heni, W.; Elder, D. L.; Korn, D.; Woessner, M.; Alloatti, L.; Koenig, S.; Schindler, P. C.; Yu, H.; Bogaerts, W.; Dalton, L. R.; Freude, W.; Leuthold, J. & Koos, C. “Femtojoule electro-optic modulation using a silicon–organic hybrid device”, *Light: Science & Applications*, Springer Science and Business Media LLC, 2015, 4, e255-e255. DOI: 10.1038/lsa.2015.28.

[16]. Kieninger, C.; Kutuvantavida, Y.; Elder, D. L.; Wolf, S.; Zwickel, H.; Blaicher, M.; Kemal, J. N.; Lauermann, M.; Randel, S.; Freude, W.; Dalton, L. R. & Koos, C. “Ultra-high electro-optic activity demonstrated in a silicon-organic hybrid modulator”, *Optica*, The Optical Society, 2018, 5, 739, DOI: 10.1364/OPTICA.5.000739